【논 문】 - 비파괴검사학회지
Journal of the Korean Society for Nondestructive Testing
Vol. 28, No. 1 (2008. 2)

Time Reversal Reconstruction of Ultrasonic Waves in Anisotropic Media

Hyunjo Jeong

Abstract Time reversal (TR) of body waves in fluids and isotropic solids has been used in many applications including ultrasonic NDE. However, the study of the TR method for anisotropic materials is not well established. In this paper, the full reconstruction of the input signal is investigated for anisotropic media using an analytical formulation, called a modular Gaussian beam (MGB) model. The time reversal operation of this model in the frequency domain is done by taking the complex conjugate of the Gaussian amplitude and phase received at the TR mirror position. A narrowband reference signal having a particular frequency and number of cycles is then multiplied and the whole signal is inverse Fourier transformed. The original input signal is seen to be fully restored by the TR process of MGB model and this model can be more generalized to simulate the spatial and temporal focusing effects due to TR process in anisotropic materials.

Keywords: Time Reversal, Anisotropic Materials, Gaussian Beam Model, Source Reconstruction

1. Introduction

The origin of the time reversal (TR) concept traces back to time reversal acoustics(Fink, 1992a, 1999b; Chakroun et al., 1995). In time reversal acoustics, an input body wave can be exactly reconstructed at the source location if a response signal measured at a distinct location is time-reversed and reemitted to the original excitation location. This phenomenon is referred to as TR of body waves and has been used in many applications including ultrasonic nondestructive evaluation and underwater communications.

While the TR method for body waves in fluids and isotropic solids has been well established (Fink and Prada, 2001; Draeger et al., 1997), the study of the TR method for anisotropic solids is relatively new. The spatial and temporal focusing effect due to the time reversal mirror (TRM) in anisotropic solid was first studied by Zhang et al. (2003) by using a ray method. The beam focusing effects will be different depending on the wave propagation direction due to the anisotropy dependence of the time reversal process of propagating waves. Thus, it is necessary to examine whether an original input signal is fully restored at the source location before the TR method is applied for anisotropic media.

In this paper, the full reconstruction of the input signal is attempted through the TR process of ultrasonic waves in anisotropic solids. To achieve this goal, a modular Gaussian beam (MGB) model is employed to simulate the TR of the longitudinal wave propagation in anisotropic solids. The MGB model provides an efficient formulation for ultrasound propagation because its properties can be described in analytical matrix form even after propagation through general anisotropic media and after interactions with multiple curved interfaces. It is shown that complete reconstruction of the original input signal can be achieved by the TR

Received: December 23, 2007, Accepted: February 5, 2008. Division of Mechanical and Automotive Engineering, Wonkwang University, 344-2 Sinyong-dong, Iksan, Jeonbuk 570-749, Korea, (E-mail: hjjeong@wonkwang.ac.kr)

process of MGB model.

2. Modular Gaussian Beam Model for Anisotropic Solids

We describe a modular Gaussian beam approach for ultrasonic beam propagation shown in Fig. 1 where a single Gaussian beam is radiated from a circular source and travels in solid media composed of two anisotropic solids and an interface. We assume the beam propagation along symmetry directions of anisotropic solids and a normal interface with respect to the beam path. For the geometry of Fig. 1, a Gaussian velocity profile for either a P-, SV- or SH-wave is present at the source and propagates as a Gaussian beam into the solid 1. In Fig. 1, $V_1(0)$ and $\mathbf{M}_1(0)$ are the known starting amplitude and phase values in the Gaussian at the source location ($\tilde{x}_3 = 0$). The propagation distance $\tilde{x}_3$ is measured along the central axis of the Gaussian beam, x_3. (x_1, x_2) are coordinates perpendicular to x_3 with x_1 in the plane of incidence and x_2 normal to that plane.

When a particular incident Gaussian beam strikes the interface, reflected and transmitted Gaussian beams are generated. For beam propagation in the symmetry direction of anisotropic solid, there is one transmitted wave of the same type as the incident wave. In order to describe the transmitted wave in the second solid we employ the coordinates (y_1, y_2, y_3), where $\tilde{y}_3$ is taken along the beam axis y_3.

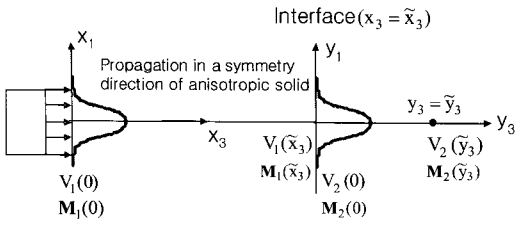

Fig. 1 Propagation of a Gaussian beam in a symmetry direction of anisotropic solid. Two anisotropic solids have a normal interface with respect to the beam path

For the geometry of Fig. 1, the particle velocity in the Gaussian beam at a distance $x_3 = \tilde{x}_3$ can be written as

$$v(\mathbf{x},\omega) = V_1(\tilde{x}_3)\ \exp\left(i\omega \left(\frac{\tilde{x}_3}{c_1} + \frac{1}{2}\mathbf{X}^T\, \mathbf{M}_1(\tilde{x}_3)\mathbf{X} \right) \right) \tag{1}$$

where $X = [x_1, x_2]^T$, ω the circular frequency, and c_1 is the phase velocity of the particular wave type in the solid 1. The amplitude $V_1(\tilde{x}_3)$ and phase $\mathbf{M}_1(\tilde{x}_3)$ of a propagating Gaussian beam can be obtained by solving the paraxial wave equation as (Schmerr and Song, 2007; Jeong and Schmerr, 2006; Jeong et al., 2005)

$$V_1(\tilde{x}_3) = \frac{V_1(0)}{\sqrt{\det[\mathbf{A}_1^P + \mathbf{B}_1^P \mathbf{M}_1(0)]}} \tag{2}$$

$$\mathbf{M}_1(\tilde{x}_3) = [\mathbf{D}_1^P\, \mathbf{M}_1(0) + \mathbf{C}_1^P][\mathbf{B}_1^P\, \mathbf{M}_1(0) + \mathbf{A}_1^P]^{-1} \tag{3}$$

where $V_1(0)$ and $\mathbf{M}_1(0)$ are the known starting amplitude and phase values in the Gaussian at the source location ($\tilde{x}_3 = 0$). The propagation matrices $(\mathbf{A}_1^P, \mathbf{B}_1^P, \mathbf{C}_1^P, \mathbf{D}_1^P)$ are given by

$$\mathbf{A}_1^P = \begin{bmatrix} 1 & 0 \\ 0 & 1 \end{bmatrix},$$

$$\boldsymbol{B}_1^P = \tilde{x}_3 \begin{bmatrix} (c_1 - 2\tilde{C}_1) & -\tilde{D}_1 \\ -\tilde{D}_1 & (c_1 - 2\tilde{E}_1) \end{bmatrix}, \tag{4}$$

$$\mathbf{C}_1^P = \begin{bmatrix} 0 & 0 \\ 0 & 0 \end{bmatrix}, \quad \mathbf{D}_1^P = \begin{bmatrix} 1 & 0 \\ 0 & 1 \end{bmatrix}$$

where the terms $(\tilde{C}_1, \tilde{D}_1, \tilde{E}_1)$ represent the slowness surface curvatures of a particular wave type in the solid 1 (as measured in the slowness coordinates (x_1, x_2, x_3)) (Jeong and Schmerr, 2006). In the isotropic case, $\tilde{C}_1 = \tilde{D}_1 = \tilde{E}_1 = 0$. These curvature terms can be obtained by expanding the x_3 component of the slowness vector, s_3, to the second order in the (x_1, x_2, x_3) coordinates (Jeong and Schmerr, 2006).

When this Gaussian beam strikes an interface, reflected and transmitted Gaussian beams are generated. The amplitude $V_2(0)$ and

polarization vector $\bar{\mathbf{d}}$ of the particular wave type transmitted in the solid 2 at the interface ($\tilde{y}_3 = 0$) in the paraxial approximation can be found by solving for the problem of the transmission of a plane wave at a planar interface. Thus, the refraction angles of transmitted waves in the solid 2 can be determined by Snell's law, and the amplitude $V_2(0)$ can be found by multiplying the incident wave by the appropriate plane wave transmission coefficient. Thus, we have

$$V_2(0) = T_{12} V_1(\tilde{x}_3) \tag{5}$$

where T_{12} is the plane wave transmission coefficient based on the velocity for an incident wave and a transmitted wave. Obtaining the phase at the interface, $\mathbf{M}_2(0)$, is more complicated. It involves matching the phases of the incident and transmitted waves at the interface and approximating the interface surface to second order (if it is curved) near the point where the central ray of the incident Gaussian strikes the interface.

$$\mathbf{M}_2(0) = [\mathbf{D}_{12}^t \mathbf{M}_1(\tilde{x}_3) + \mathbf{C}_{12}^t][\mathbf{B}_{12}^t \mathbf{M}_1(\tilde{x}_3) + \mathbf{A}_{12}^t]^{-1} \tag{6}$$

where the transmission matrices $(\mathbf{A}_{12}^t, \mathbf{B}_{12}^t, \mathbf{C}_{12}^t, \mathbf{D}_{12}^t)$ are given by

$$A_{12}^t = \begin{bmatrix} 1 & 0 \\ 0 & 1 \end{bmatrix}, \quad B_{12}^t = \begin{bmatrix} 0 & 0 \\ 0 & 0 \end{bmatrix}, \quad C_{12}^t = \begin{bmatrix} 0 & 0 \\ 0 & 0 \end{bmatrix}, \quad D_{12}^t = \begin{bmatrix} 1 & 0 \\ 0 & 1 \end{bmatrix} \tag{7}$$

Similar expressions can be obtained for the interface reflection by modifying the transmission matrices, although not shown here.

In the solid 2, the propagation laws for a particular wave type (Gaussian amplitude and phase, $V_2(\tilde{y}_3)$ and $\mathbf{M}_2(\tilde{y}_3)$), follow the same law as in the solid 1.

$$V_2(\tilde{y}_3) = \frac{V_2(0)}{\sqrt{\det[\mathbf{A}_2^P + \mathbf{B}_2^P \mathbf{M}_2(0)]}} \tag{8}$$

$$\mathbf{M}_2(\tilde{y}_3) = [\mathbf{D}_2^p \mathbf{M}_2(0) + \mathbf{C}_2^p][\mathbf{B}_2^p \mathbf{M}_2(0) + \mathbf{A}_2^p]^{-1} \tag{9}$$

The propagation matrices $(\mathbf{A}_2^p, \mathbf{B}_2^p, \mathbf{C}_2^p, \mathbf{D}_2^p)$ in the solid 2 are given by

$$\mathbf{A}_2^p = \begin{bmatrix} 1 & 0 \\ 0 & 1 \end{bmatrix}, \quad \boldsymbol{B}_2^P = \tilde{y}_3 \begin{bmatrix} (c_2 - 2\tilde{C}_2) & -\tilde{D}_2 \\ -\tilde{D}_2 & (c_2 - 2\tilde{E}_2) \end{bmatrix},$$

$$\mathbf{C}_2^p = \begin{bmatrix} 0 & 0 \\ 0 & 0 \end{bmatrix}, \quad \mathbf{D}_2^p = \begin{bmatrix} 1 & 0 \\ 0 & 1 \end{bmatrix} \tag{10}$$

Finally the velocity field of the Gaussian beam at a distance $y_3 = \tilde{y}_3$ is given by

$$v(\mathbf{x}, \omega) = V_2(\tilde{y}_3) \exp\left(i\omega \left(\frac{\tilde{x}_3}{c_1} + \frac{\tilde{y}_3}{c_2} + \frac{1}{2} \mathbf{Y}^T \mathbf{M}_2(\tilde{y}_3) \mathbf{Y} \right) \right) \tag{11}$$

where $\boldsymbol{Y} = [y_1, y_2]^T$

3. Time Reversal Simulation for Anisotropic Solids

In this section, a numerical experiment is executed to demonstrate the applicability of the time reversal method to elastic wave phenomena in anisotropic solids. As an example of the use of this method, we consider a unidirectional graphite/epoxy composite whose properties are assumed to be transversely isotopic: C_{11}=C_{22}=15, C_{12}=7.7, C_{13}=C_{23}=3.4, C_{33}=87, C_{44}=C_{55}=7.8, C_{66}=3.65 GPa and ρ=1.595 g/cm^3. Consider a quasilongitudinal (qL) wave Gaussian beam radiating from a source (5 MHz, 4.763 mm radius planar transducer) directly into the solid along the x_3 axis, an axis of symmetry. Under this condition, the slowness surface curvatures are $\tilde{C}_1 = \tilde{C}_2 = \tilde{D}_1 = \tilde{D}_2 = 3.3$ mm/μs, and $\tilde{D}_1 = \tilde{D}_2 = 0$ (Jeong and Schmerr, 2007). The time reversal mirror (TRM) is located at $\tilde{x}_3 = 50$ mm in Fig. 1. Once a response signal is measured at the TRM, the reconstructed signal at the source can be obtained by reemitting the time-reversed response signal at the TRM. Thus, the time reversal operation of this model in the frequency

domain is done by taking the complex conjugate of the Gaussian amplitude and phase received at the TRM position. Therefore, the reconstructed signal at the source location from the reemitted signal from the TRM can be written as

$$v_{TR}(\mathbf{x},\omega) = \frac{V_1^*(\tilde{x}_3)}{\sqrt{\det\left[\mathbf{A}_2^p + \mathbf{B}_2^p \mathbf{M}_2(0)\right]}} \exp\left(\frac{i\omega}{2}\mathbf{Y}^T \mathbf{M}_2^*(\tilde{y}_3)\mathbf{Y}\right) \quad (12)$$

where a superscript * denotes a complex conjugate. If the TR of a wave is satisfied, the reconstructed time domain signal $v_{TR}(t)$ in eqn. (12) would be identical to the time-reversed original input signal $v_s(T-t)$ where T represents the total time duration of the signal. To directly compare with the original input signal $v_s(t)$ at the source, an inverse Fourier transform of eqn. (12) should be time reversed, thus

$$v_{TR}(T-t) = \frac{1}{2\pi}\int_{-\infty}^{\infty} v_{TR}(\mathbf{x},\omega)\, e^{-i\omega(T-t)}\, d\omega \quad (13)$$

The simulation results for the qL wave case are shown in Fig. 2. A narrowband (toneburst) reference signal of center frequency f=5 MHz and N=5 cycles (Fig. 2(a)) is used to simulate an actual signal waveform in the time domain. Shown in Fig. 2(b) is the time domain input signal calculated at the center of the circular Gaussian beam. Fig. 2(c) is the received signal at the TRM position ($\tilde{x}_3$=50 mm), where the arrival time of the qL wave, about 67.7 μs, is seen to be correct. Fig. 2(d) shows comparisons, after normalization by its maximum amplitude,

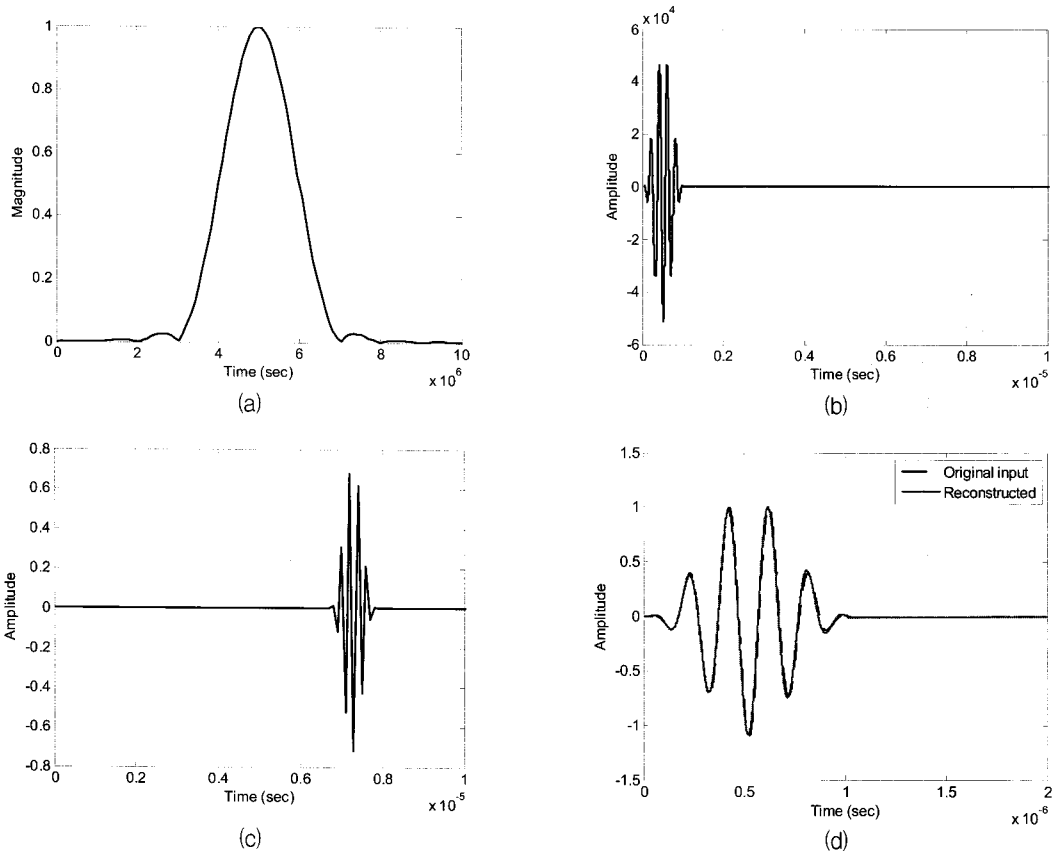

Fig. 2 Time reversal process of qL wave using a single Gaussian beam source and a narrowband toneburst reference signal. (a) magnitude spectrum of the reference signal, (b) time domain input signal at the center of the Gaussian beam, (c) received signal at the TRM position ($\tilde{x}_3$=50 mm), and (d) reconstructed TR signal and comparison with the original input signal

between the original input signal and the reconstructed TR toneburst waveform by the TR process. When the response signal (Fig. 2(c)) is reversed in time and reemitted to the source, the shape of the original input signal is seen to be fully recovered. This result indicates that the MGB model can be an efficient tool for simulating other TR processes for anisotropic materials.

4. Coclusions

The MGB model was used to simulate a simple TR process for anisotropic materials and it was shown that complete reconstruction of the original input signal could be achieved by the TR process of this model. The present MGB model can also be applied to simulate other TR processes for anisotropic solids: longer propagation distances, broadband pulse shape for the input and reconstructed TR signal waveforms, arbitrary propagation directions with multiple curved interfaces.

Ultrasonic inspections using array type sensors are widely employed to enhance flaw detectability through beam focusing and steering. The MGB model used in this study can be more generalized to simulate the spatial and temporal focusing effects by TR array sensors for anisotropic materials as well as fluids and isotropic solids.

Acknowledgement

This work was supported by the Korea Science and Engineering Foundation (KOSEF) grant for the year 2007 funded by the Korea government (MOST).

References

Chakroun, N., Fink, M. and Wu, F. (1995) Time Reversal Processing in Ultrasonic Nondestructive Testing, *IEEE Trans. UFFC* Vol. 42, pp. 1087

Draeger, C., Cassereau, D. and Fink, M. (1997) Acoustic Time Reversal in Solids, *J. Acoust. Soc. Am.* Vol. 102, No. 3, pp. 1289-1295

Fink, M. (1992) Time Reversal of Ultrasonic Fields: part I. Basic principles, *IEEE Trans. UFFC* Vol. 39, pp. 555-566

Fink, M. (1999) Time-Reversed Acoustics, *Scientific American* Vol. 281, pp. 91-97

Fink, M. and Prada, C. (2001) Acoustic Time-Reversal Mirrors, *Inverse Problems* Vol. 17, R1-R38

Jeong, H. and Schmerr, L. W. Jr. (2006) Effects of Material Anisotropy on Ultrasonic Beam Propagation: Diffraction and Beam Skew, *Journal of the Korean Society for Nondestructive Testing*, Vol. 26, No. 3, pp. 198-205

Jeong, H., Park, M.-C. and Schmerr, L. W. Jr. (2005) Application of a Modular Multi-Gaussian Beam Model to Ultrasonic Wave Propagation with Multiple Interfaces, *Journal of the Korean Society for Nondestructive Testing*, Vol. 25, No. 3, pp. 163-170

Jeong, H. and Schmerr, L. W. Jr. (2007) Ultrasonic Beam Propagation in Highly Anisotropic Materials Simulated by Multi-Gaussian Beams, *Mechanical Science and Technology* Vol. 21, pp. 1139-1149

Schmerr, L. W. Jr. and Song, S.-J. (2007) *Ultrasonic NDE Systems: Models and Measurements,* Springer

Zhang, B., Wang, C. and Lu, M. (2003) Time Reversal Self-Adaptive Focusing in Anisotropic Elastic Solid Medium, *Acoustical Physics* Vol. 49, No. 6, pp. 688-694